

## Autoresonant Transition in the Presence of Noise and Self-Fields

I. Barth,<sup>1,†</sup> L. Friedland,<sup>1,\*</sup> E. Sarid,<sup>2</sup> and A. G. Shagalov<sup>3</sup>

<sup>1</sup>Racah Institute of Physics, Hebrew University of Jerusalem, Jerusalem 91904, Israel

<sup>2</sup>Department of Physics, NRCN-Nuclear Research Center Negev, Beer Sheva, 84190, Israel

<sup>3</sup>Institute of Metal Physics, Ekaterinburg 620219, Russian Federation

(Received 26 June 2009; published 7 October 2009)

A sharp threshold for resonant capture of an ensemble of trapped particles driven by chirped frequency oscillations is analyzed. It is shown that at small temperatures  $T$ , the capture probability versus driving amplitude is a smoothed step function with the step location and width scaling as  $\alpha^{3/4}$  ( $\alpha$  being the chirp rate) and  $(\alpha T)^{1/2}$ , respectively. Strong repulsive self-fields reduce the width of the threshold considerably, as the ensemble forms a localized autoresonant macroparticle.

DOI: 10.1103/PhysRevLett.103.155001

PACS numbers: 52.35.Mw, 52.27.Jt

The capture of an oscillatory nonlinear system into resonance by chirped frequency perturbations is an important process in planetary dynamics [1] and many applications ranging from atomic physics [2,3] and plasmas [4–6] to fluid dynamics [7], Bose-Einstein condensates [8], and nonlinear waves [9,10]. After the capture into resonance, the system may remain phase locked to the drive continuously despite variation of the driving frequency. Such an autoresonant state is efficiently controlled by external parameters, a famous example being acceleration of particles in cyclotron accelerators by chirped frequency drives [11,12]. There are two different limits of passage through and capture into a nonlinear resonance. One corresponds to the case of an oscillatory system excited to a large amplitude initially. In this case, for a small driving amplitude  $\varepsilon$ , only a small fraction of initial phases of oscillations is captured into resonance, suggesting a probabilistic approach to the problem [13]. In contrast, when passing through resonance with zero amplitude equilibrium, there exists a sharp transition to autoresonance (AR) if the driving amplitude exceeds a critical value, scaling as  $\varepsilon_{cr} \propto \alpha^{3/4}$  ( $\alpha$  being the driving frequency chirp rate) [14]. Above  $\varepsilon_{cr}$ , the system is captured into AR regardless of the initial phase of the drive and may reach large excitations as the variation of the driving frequency continues. In contrast, below  $\varepsilon_{cr}$ , no phase locking is observed and the excitation level remains small. In recent years, this sharp threshold transition to AR served as a powerful approach to excitation and control of a variety of nonlinear waves and oscillations [15]. However, for a distribution of initial conditions near the equilibrium, a finite width of the threshold was seen in planetary dynamics simulations [16,17]. A similar broadening of the width of the threshold was also observed in recent superconducting Josephson resonator experiments [18], the effect associated with the noise in the system. In this Letter, for the first time, we address the problem of the width of the autoresonant transition analytically, focusing on noisy nonlinear oscillators and Penning-trapped nonneutral plasmas. The par-

ticles bouncing along the magnetic field in these plasmas comprise an ensemble of nonlinear oscillators; however, in addition to the thermal noise, one must include the repulsion of the plasma cloud due to the self-fields. We will show that, counterintuitively, after passage through resonance, these repulsive fields may assist the plasma to bunch and form an autoresonant macroparticle, narrowing the width of the AR transition significantly.

Consider a driven nonlinear damped oscillator

$$\ddot{x} + \nu \dot{x} + \sin x = \varepsilon \cos \psi_d + \xi_0 \xi(t), \quad (1)$$

where  $x$ , time  $t$ , and all parameters are dimensionless,  $\psi_d = \int \omega_d dt$  is the phase of a chirped frequency ( $\omega_d = 1 - \alpha t$ ) drive,  $\xi(t)$  is a delta correlated Gaussian noise,  $\langle \xi(0) \xi(t) \rangle = \delta(t)$ , and the equilibrium temperature  $T = \xi_0^2 / 2\nu$  is given by the fluctuation-dissipation theorem. Figure 1 shows the numerical AR capture probability [fraction of realizations of Eq. (1) leading to phase locking] versus the rescaled driving amplitude  $\mu$  [see the definition

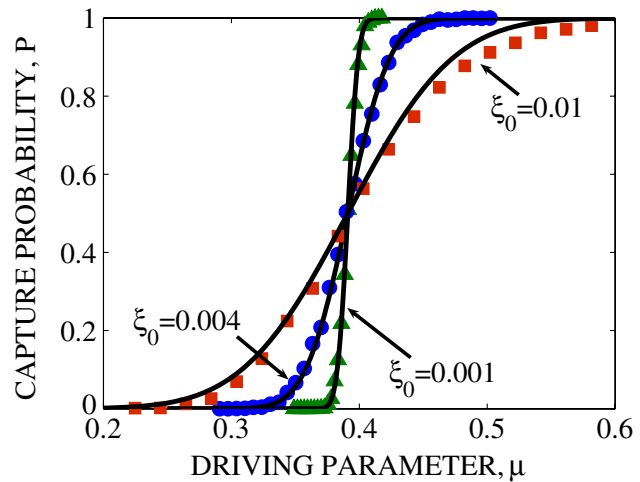


FIG. 1 (color online). Autoresonant capture probability versus driving parameter  $\mu$  at different noise levels  $\xi_0$ . The solid lines show theoretical predictions.

below Eq. (3)] as the driving frequency passes the linear resonance from above by starting at a large negative time. The parameters in these simulations are  $\nu = 0.001$ ,  $\alpha = 0.002$ , and three different temperatures in the figure correspond to  $\xi_0 = 0.01$ ,  $0.004$ , and  $0.001$ . One observes a nearly complete phase-locking transition beyond some critical  $\mu$ ; the increase of the width of this transition with temperature is also observed. The solid lines in Fig. 1 represent the results from our theory developed below. A similar qualitative dependence of the capture probability was obtained in simulations in planetary dynamics [16] and Josephson junction experiments [18].

Our theory assumes a sufficiently small temperature case, allowing a weakly nonlinear description [ $\sin x \approx x - \beta x^3$  ( $\beta = 1/6$ ) in Eq. (1)] of the resonant capture process. We also assume that the passage through the resonance is sufficiently fast so that the effect of the noise on the dynamics during the resonant capture process can be neglected. This allows us to replace Eq. (1) with a deterministic system (neglecting the noise term) with random initial conditions formed due to the combined effect of noise and dissipation at earlier times. After the capture into AR, the effect of the noise can also be neglected, provided the escape time [19] due to the noise from the resonant bucket is sufficiently large (the analysis of this problem is out of the scope of the present work). These approximations were satisfied in our numerical examples in Fig. 1, showing a good agreement between the resulting theory and simulations with the drive switched on after a sufficient initial time, allowing development of a steady distribution of initial conditions. The probability of capture into AR (Fig. 1) can be calculated by averaging the outcome of passage through resonance over this initial thermal distribution. For the analysis, we neglect the stochastic term in the weakly nonlinear version of Eq. (1), seek solutions of form  $x = a \cos \theta$  ( $a$  and  $d\theta/dt$  are slow objects in the theory), use the single resonance approximation (i.e., view the phase mismatch  $\phi = \theta - \phi_d$  as a slow variable and neglect nonresonant terms), and average over the fast phase variable  $\theta$ , yielding a slow system for  $a$  and  $\phi$ :

$$\dot{a} = -\frac{\nu}{2}a - \frac{\varepsilon}{2} \sin \phi, \quad (2)$$

$$\dot{\phi} = \frac{3}{8}\beta a^2 - \alpha t - \frac{\varepsilon}{2a} \cos \phi. \quad (3)$$

Next, we rescale the time,  $\tau = \sqrt{\alpha}t$ , define  $\gamma = \frac{\nu}{2\sqrt{\alpha}}$ ,  $\mu = (\sqrt{3\beta/2\varepsilon})/(4\alpha^{3/4})$ , and  $A = \sqrt{3\beta/8\alpha^{-1/4}}a$ , and introduce a complex dependent variable,  $\Psi = Ae^{i\phi}$ . Then, Eq. (3) reduces to a nonlinear Schrödinger-type equation:

$$i\dot{\Psi} + (|\Psi|^2 - \tau)\Psi + i\gamma\Psi = \mu. \quad (4)$$

Subject to zero initial condition, this two parameter  $(\mu, \gamma)$  equation yields a sharp threshold transition to AR at  $\mu > \mu_{\text{cr}}$ , i.e., to  $|\Psi|^2 = A^2 \approx \tau$ ,  $\phi \approx 0$  at large positive  $\tau$ , while the critical parameter  $\mu_{\text{cr}}$  depends on  $\gamma$  [18]. In

contrast, for nonzero initial conditions,  $\mu_{\text{cr}}$  depends on the initial amplitude and phase mismatch,  $\mu_{\text{cr}} = \mu_{\text{cr}}(\gamma, A_0, \phi_0)$ . This  $\mu_{\text{cr}}$  is periodic in  $\phi_0$  and can therefore be expanded in Fourier series  $\mu_{\text{cr}}(\gamma, A_0, \phi_0) = c_0 + c_1 \cos(\phi_0 + \delta) + \dots$ . We found in simulations that for initial amplitudes  $A_0 < 0.3$ , only the zeroth and first harmonic in the expansion were significant. Since  $\mu_{\text{cr}}$  is independent of  $\phi_0$  for  $A_0 = 0$ ,  $c_1$  is of  $O(A_0)$  and therefore to lowest order in  $A_0$ ,

$$\mu_{\text{cr}}(\gamma, A_0, \phi_0) \approx c_0 + \kappa A_0 \cos(\phi_0 + \delta), \quad (5)$$

where the coefficients  $c_0$  and  $\kappa$  can be found numerically. Typically, for small values of  $\gamma$  and  $A_0$ ,  $c_0$  is near 0.4 [18]. For example, in Fig. 1 with  $\nu = 0.001$ , one finds  $c_0 = 0.395$  and  $\kappa = 0.245$ . Higher harmonics in the Fourier expansion for  $\mu_{\text{cr}}$  must be included in the theory for  $A_0 > 0.3$ . Next, we calculate the probability  $P(A_0, \mu, \gamma)$  for capture into resonance for fixed  $A_0$  and uniformly distributed initial phase mismatch  $\phi_0$ . The interval of initial  $\phi_0$  leading to trapped trajectories for given  $\mu$  is  $\Delta\phi_0 = \arccos[(c_0 - \mu)/(\kappa A_0)]$  [see Eq. (5)]. Then,  $P = 0$  for  $(\mu - c_0) < -\kappa A_0$ ,  $P = (1/\pi) \arccos[(c_0 - \mu)/(\kappa A_0)]$  for  $|\mu - c_0| < \kappa A_0$ , and  $P = 1$  for  $(\mu - c_0) > \kappa A_0$ . We integrate this result over the thermal distribution  $f(A_0) = \sigma^{-2} A_0 \exp(-A_0^2/2\sigma^2)$  of the initial amplitudes [with  $\sigma^2 = (3\beta T)/(8\sqrt{\alpha})$  and  $T$  defined in Eq. (1)], yielding the resonant capture probability  $P(\mu) = \int_0^\infty P(A_0, \mu) \times f(A_0) dA_0$ , which is in good agreement with simulations in Fig. 1. Finally, upon differentiation of  $P(\mu)$ , one finds the slope  $S = (\sqrt{2\pi}\sigma\kappa)^{-1}$  of the transition probability at the central value  $\mu = c_0$ . Thus, in terms of the original driving amplitude, the location of the phase-locking transition and its width scale as  $\alpha^{3/4}$  and  $(\alpha T)^{1/2}$ , respectively. This result can be used in applications (e.g., [18]) for temperature or noise level diagnostics. Note that our theoretical predictions are in excellent agreement with simulations in Fig. 1 for the two lowest temperatures. At the highest temperature, the average initial amplitude was 0.33, violating our small amplitude assumption, and the agreement with the simulations is not as good. Note that we did not discuss the physical reasons for the thermal broadening of the phase-locking transition. We will relate the effect later to a parametric resonance in the problem.

The problem of finding the probability of capture into resonance for a noisy oscillator is equivalent to that of calculating the fraction of AR trapped particles in a dilute thermally distributed nonneutral plasma in an electrostatic trap if one neglects the repulsive self-field. However, as the density of the plasma increases, the question of the effect of the self-field becomes important and is addressed next. We focus on a single species plasma column surrounded by a cylindrical wall of radius  $R$ . The plasma is radially confined by an axial magnetic field and longitudinally trapped in an external electrostatic potential for which we choose the form  $V(x) = V_0[1 - \cos(2\pi x/L)]$ ,  $x$  being in the direction of the magnetic field. We perturb this

plasma by an oscillating chirped frequency potential  $\varphi^d = -\varepsilon x \cos \psi_d$  and model the associated driven kinetic problem by the 1D Vlasov equation for the normalized distribution function  $f(u, x, t)$ :

$$f_t + u f_x - (V + \varphi + \varphi^d)_x f_u = D f_{uu}, \quad (6)$$

where the diffusion term in velocity space is introduced to deal with numerical singularities characteristic of the Vlasov solver in the case of interest [see the distributions in Figs. 2(a) and 2(b)] and  $\varphi(x)$  is the self-potential satisfying the Poisson equation

$$\varphi_{xx} = \chi^2 \varphi - \eta^2 \int f(u, x, t) du. \quad (7)$$

Here, we assume a positively charged plasma of unperturbed ( $\varphi = 0$ ) central density  $n_0$ , use the dimensionless coordinate  $x$ , time  $t$ , and velocity  $u$  expressed in units of  $L/2\pi$ ,  $\omega_0^{-1} = (L/2\pi)(eV_0/m)^{-1/2}$ , and  $(eV_0/m)^{1/2}$ , respectively. The dimensionless potentials  $\varphi$ ,  $\varphi_d$ , and  $V$  in Eqs. (6) and (7) are expressed in units of  $V_0$ . The radial decay of the self-potential in the trap is modeled by the screening term  $\chi^2 \varphi$ , where  $\pi\chi = L/R$  is the aspect ratio, while  $\eta = \omega_p/\omega_0$  and  $\omega_p = (4\pi e^2 n_0/m)^{1/2}$  is the plasma frequency. We followed the evolution of the distribution function of the driven plasma by solving this Vlasov-Poisson system numerically. Our Vlasov solver used the pseudospectral algorithm described in [20]. The initial distribution was  $f(u, x, 0) = \sqrt{\rho/2\pi} \exp\{-\rho[u^2/2 + V(x) + \varphi_0(x) - \varphi_0(0)]\}$ , where  $\rho = eV_0/(k_B T)$  and  $\varphi_0(x)$  was the initial self-potential, satisfying the stationary unperturbed Vlasov-Poisson system. Figures 2(a), 2(c), and 2(d) show the snapshots of  $f(u, x, t)$  after passage through resonance for  $\varepsilon = 0.0156$ ,  $\alpha = 8 \times 10^{-4}$ , and three different initial plasma densities. Figure 2(a) corresponds to the low density plasma case with  $\eta^2 = 0.1$ ,  $\chi^2 = 10$ , and  $D = 2.25 \times 10^{-5}$ . The initial distribution at  $t = -150$  had  $\rho = 50$ , and the final distribution at  $t = 300$  is

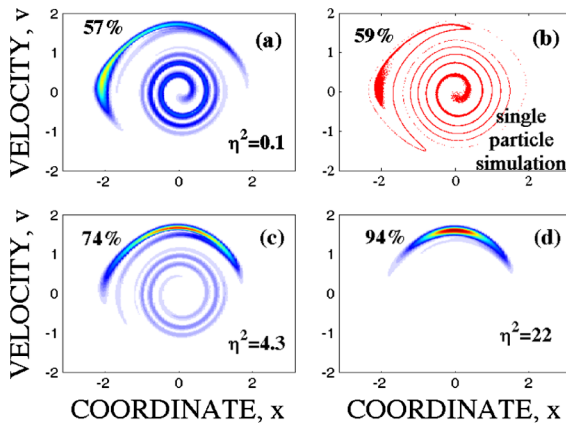


FIG. 2 (color online). Snapshots of distribution after passage through resonance for different plasma densities (a)  $\eta^2 = 0.1$ , (c)  $\eta^2 = 4.3$ , and (d)  $\eta^2 = 22$ . (b) Single particle simulation. Percentage indicates the fraction of trapped particles.

shown in the figure. For comparison, we have performed single particle (neglecting self-fields) simulations for the same parameters and initial conditions and show the results in Fig. 2(b). Each point in this figure corresponds to a final position of the trajectory in phase space with Monte Carlo simulated initial conditions chosen from the initial distribution. We found that 59% of the plasma species were captured into resonance in this case [see Fig. 2(a)], while the remaining particles stayed in a spiral pattern near the equilibrium. Note that due to the diffusion term, the Vlasov simulation in Fig. 2(a) yields a smoothed distribution but preserves its general shape in phase space and the number of particles in the trapped and untrapped groups, yielding (in the case of small  $\eta^2$ ) nearly the same capture probability as in the single particle simulation in Fig. 2(b). The intermediate and high density cases,  $\eta^2 = 4.3$  and 22, are illustrated in Figs. 2(c) and 2(d) for the remaining parameters as in Fig. 2(a). We observe that nearly all particles in the  $\eta^2 = 22$  case are trapped in resonance at the final time and that the distribution is compact; i.e., the plasma evolves as an autoresonant macroparticle, which is phase locked to the drive continuously despite the variation of the driving frequency. As a result, the macroparticle increases its energy with the decrease of the driving frequency, and the plasma location in phase space and its phase relative to the drive are efficiently controlled. Additional results of our Vlasov-Poisson simulations are presented in Fig. 3, showing the AR capture probabilities versus the driving amplitude. This figure is similar to Fig. 1 but represents three different plasma densities instead of different temperatures. We used the same  $\chi^2$ ,  $\rho$ , and  $D$  as above and  $\eta^2 = 0.1$ , 4.3, and 22 (in the case of  $\eta^2 = 22$ , these parameters could correspond to a positron plasma of  $n_0 = 4.8 \times 10^7 \text{ cm}^{-3}$  and  $k_B T = 0.2 \text{ eV}$  in the trap with  $L = 10 \text{ cm}$ ,  $R = 1.0 \text{ cm}$ , and  $eV_0 = 10 \text{ eV}$ ). One can see in Fig. 3 that despite the growing (with density) repulsive self-potential, the width of the AR transition narrows as the particles tend to bunch together in the case of strong self-

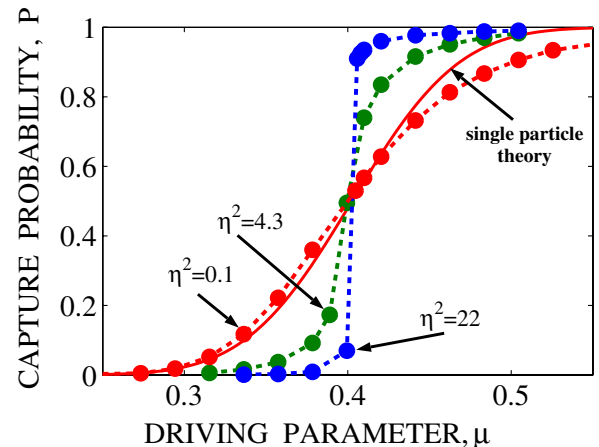


FIG. 3 (color online). Autoresonant capture probability for a driven trapped nonneutral plasma versus driving parameter  $\mu$  at different plasma densities (parameter  $\eta^2$ ).

fields [as in Fig. 2(d)]. In contrast, for small self-fields ( $\eta^2 = 0.1$ ), we nearly reproduce the result of our single particle theory, shown by the solid line in Fig. 3. This effect of the self-field on the width of the AR transition is discussed next.

Assume a continuing clustering of the plasma in AR around the time dependent centroid  $x_0(t)$ , as observed in simulations for a sufficiently large plasma density. Assume also that the spatial distribution of the charge in the bunch is symmetric around  $x_0$ . Then, the self-potential will be an even function  $\varphi(\xi)$ , where  $\xi = x - x_0(t)$ . The dynamics of a test particle in such a bunch is governed by  $x_{tt} = -\sin x - \varphi_x + \varepsilon \cos \psi_d$ , where we expand  $\sin x$  to first order in  $\xi$  to get  $\xi_{tt} = -x_{0tt} - \sin x_0 - \xi \cos x_0 - \varphi_\xi + \varepsilon \cos \psi_d$ . We define the centroid  $x_0(t)$  by the equation  $x_{0tt} = -\sin x_0 + \varepsilon \cos \psi_d$  describing a quasiparticle in our external potential and driven by the chirped frequency drive. The solution of this problem is known [15], and if the driving amplitude exceeds the threshold, the centroid is captured into AR, i.e.,  $x_0 \approx a(t) \cos \psi_d$  in the weakly nonlinear limit, with the amplitude  $a(t)$  growing in time to maintain the phase locking in the system. The position of a test particle relative to  $x_0(t)$  in this case is governed by  $\xi_{tt} \approx -[(1 - \frac{1}{4}a^2)\xi^2/2 + \varphi]_\xi + \frac{1}{4}\xi a^2 \cos 2\psi_d$ . This equation comprises a parametrically driven nonlinear oscillator problem in a slowly varying combined external and self-potential  $\varphi_{\text{eff}} \approx \xi^2/2 + \varphi$ . For small  $\xi$ , we expect stable oscillations in this problem, unless the driving term resonates with the natural oscillation frequency  $\omega_{\text{eff}}$  in the combined potential, i.e.,  $\omega_d \approx \omega_{\text{eff}}$ . Here enters the effect of the symmetric self-potential, which, because of its repulsive nature, has a negative parabola form  $\varphi \approx -k\xi^2/2$  ( $k > 0$ ) at small  $\xi$ . As the result,  $\omega_{\text{eff}}$  decreases when one includes the self-field and the parametric resonance is avoided if the field is sufficiently strong. In such a case, stable oscillations of  $\xi$  around the autoresonant centroid explain the assumed symmetry of the plasma charge around  $x_0(t)$  and the preservation of the tight bunching of the plasma. In contrast, at low densities,  $\varphi \approx 0$ , and we return to the single particle case discussed above. In this limit,  $\omega_{\text{eff}} \approx \omega_d \approx 1$ , as the drive passes the linear resonance. Consequently, the parametric resonance destroys the initial localization of the ensemble in phase space, broadening the width of the phase-locking transition.

In summary, we have presented a theory describing the shape and the width of the AR phase-locking transition versus the driving amplitude for both stochastic oscillators and dilute nonneutral plasmas in Penning traps driven by chirped frequency drives. We have also observed and explained how the inclusion of the repulsive self-field in the problem yields a continuing particle bunching in the driven trapped nonneutral plasma case and a significant narrowing of the AR phase-locking transition width. The plasma in this case behaves as an autoresonant macroparticle and can

be efficiently controlled by external parameters. Our theory agrees with simulations for the driven oscillators in the presence of thermal noise as well as with Vlasov-Poisson simulations. Applications of these results to nonneutral plasmas could include (a) longitudinal (with respect to the direction of the magnetic field) autoresonant plasma manipulation in cryogenic Penning traps aimed at formation and trapping of antihydrogen atoms [21,22] and (b) the problem of precise transverse positron plasma (diocotron mode) positioning for storage in multicell traps [6]. It seems important to further develop the theory for handling the autoresonant capture problem in the case of intermediate plasma densities, including the details of destruction of the plasma macroparticle via the parametric resonance.

This work was supported by the Israel Science Foundation (Grant No. 1080/06).

\*lazar@vms.huji.ac.il

<sup>†</sup>ido.bARTH@mail.huji.ac.il

- [1] R. Malhotra, Nature (London) **365**, 819 (1993).
- [2] W. K. Liu, B. R. Wu, and J. M. Yuan, Phys. Rev. Lett. **75**, 1292 (1995).
- [3] H. Maeda, J. Nunkaew, and T. F. Gallagher, Phys. Rev. A **75**, 053417 (2007).
- [4] M. Deutsch, B. Meerson, and J. E. Golub, Phys. Fluids B **3**, 1773 (1991).
- [5] J. Fajans, E. Gilson, and L. Friedland, Phys. Plasmas **6**, 4497 (1999).
- [6] J. R. Danielson, T. R. Weber, and C. M. Surko, Phys. Plasmas **13**, 123502 (2006).
- [7] L. Friedland, Phys. Rev. E **59**, 4106 (1999).
- [8] A. I. Nicolin, M. H. Jensen, and R. Carretero-Gonzalez, Phys. Rev. E **75**, 036208 (2007).
- [9] I. Aranson, B. Meerson, and T. Tajima, Phys. Rev. A **45**, 7500 (1992).
- [10] L. Friedland and A. G. Shagalov, Phys. Rev. E **71**, 036206 (2005).
- [11] E. M. McMillan, Phys. Rev. **68**, 143 (1945).
- [12] V. I. Veksler, J. Phys. USSR **9**, 153 (1945).
- [13] See A. Neishtadt and A. Vasiliev, Phys. Rev. E **71**, 056623 (2005), and references therein.
- [14] See L. Friedland, J. Phys. A **41**, 415101 (2008), and references therein.
- [15] L. Friedland, Scholarpedia **4**, 5473 (2009).
- [16] M. C. Wyatt, Astrophys. J. **598**, 1321 (2003).
- [17] A. C. Quillen, Mon. Not. R. Astron. Soc. **365**, 1367 (2006).
- [18] O. Naaman, J. Aumentado, L. Friedland, J. S. Wurtele, and I. Siddiqi, Phys. Rev. Lett. **101**, 117005 (2008).
- [19] C. W. Gardiner, *Handbook of Stochastic Methods* (Springer-Verlag, Berlin, 1985).
- [20] L. Friedland, P. Khain, and A. G. Shagalov, Phys. Rev. Lett. **96**, 225001 (2006).
- [21] G. Andresen *et al.*, Phys. Rev. Lett. **98**, 023402 (2007).
- [22] G. Gabrielse *et al.*, Phys. Rev. Lett. **98**, 113002 (2007).